Journal of Power Sources 196 (2011) 2545–2550

Contents lists available at ScienceDirect

Journal of Power Sources

journal homepage: www.elsevier.com/locate/jpowsour

Syngas reactivity over $(LaAg)(CoFe)O_3$ and Ag-added $(LaSr)(CoFe)O_3$ anodes of solid oxide fuel cells

Ta-Jen Huang*, Chi-Mei Chen

Department of Chemical Engineering, National Tsing Hua University, Hsinchu 30013, Taiwan, ROC

ARTICLE INFO

Article history:
Received 19 October 2010
Received in revised form 2 November 2010
Accepted 3 November 2010
Available online 9 November 2010

Keywords:
Syngas
Reactivity
Perovskite
Anode
Silver
Solid oxide fuel cell

ABSTRACT

The syngas, H_2 + CO gas mixture with various H_2/CO ratios, is used as the anode fuel of solid oxide fuel cell with $La_{0.7}Ag_{0.3}Co_{0.2}Fe_{0.8}O_3$ (LACF) and 2 wt% Ag-added $La_{0.58}Sr_{0.4}Co_{0.2}Fe_{0.8}O_3$ (LSCF) as the anode, respectively, both being in composite with 50 wt% $Ce_{0.9}Gd_{0.1}O_{1.95}$ (GDC). Both the current–voltage and the fixed-voltage measurements are performed at 800 °C. The reactivity with H_2 as the fuel is larger than that with CO. The syngas reactivity increases with increasing H_2 content. The results of the current–voltage and the fixed-voltage measurements are in agreement with each other. Ag-added LSCF–GDC has better reactivity with H_2, CO and syngas and better stability in the H_2 atmosphere than LACF–GDC as the anode material.

1. Introduction

Coal is an abundant and low cost fuel and will be used in power generation for years to come. The technology for coal gasification allows the environmental-friendly use of coal for power generation; coal gasification by steam produces the coal gas:

$$C + H_2O \rightarrow CO + H_2 \quad (1)$$

Thus, the use of coal syngas as the anode fuel for solid oxide fuel cells (SOFCs) has gained increasing research interest [1–8]. On the other hand, various hydrocarbon fuels have been used for the SOFCs; these fuels are usually processed before such usage to avoid or reduce the problem of carbon deposition. The fuel processing technologies are, taking methane as an example of the fuels:

Steam reforming:

$$CH_4 + H_2O \rightarrow CO + 3H_2 \quad (2)$$

CO_2 reforming:

$$CH_4 + CO_2 \rightarrow 2CO + 2H_2 \quad (3)$$

Partial oxidation:

$$CH_4 + O_2 \rightarrow CO + H_2 + H_2O \quad (4)$$

All these reactions produce the syngas—that is, a gas mixture of H_2 and CO with various H_2/CO ratios. Additionally, since hydrogen is the most efficient fuel for the SOFCs, water–gas shift reaction is usually carried out to convert CO to hydrogen:

$$CO + H_2O \rightarrow CO_2 + H_2 \quad (5)$$

This increases the H_2/CO ratio in the syngas. Therefore, the SOFCs actually deal with the (H_2 + CO) gas mixture, the syngas, as the reactant over the anodes and the knowledge on the syngas reactivity over the SOFC anodes should be important. However, the syngas reactivity in the SOFCs is seldom studied.

Coal syngas reactivity in the SOFCs has been studied by Huang et al. [9] with Ni-added $La_{0.58}Sr_{0.4}Co_{0.2}Fe_{0.8}O_3$–gadolinia-doped ceria composite as the anode; the maximum power density with pure CO as the anode fuel is higher than that with pure H_2 and increases as the CO content in the CO + H_2 mixture increases. For this case, higher SOFC performance would demand a fuel processing to produce a syngas with smaller H_2/CO ratio. Thus, it should be interesting to study other SOFC anodes to see whether the effect of the H_2/CO ratio on the syngas reactivity is the same or not; this would change the strategy of fuel processing.

The $(LaSr)(CoFe)O_3$ (LSCF) perovskites have been studied as the anode materials for the SOFCs [10]. Other La and Sr based perovskites have also been studied as the SOFC anode materials to have an enhanced anodic activity [11,12]. On the other hand, gadolinia-doped ceria (GDC) is the well-known materials in the SOFC anodes [13]. The mixing of GDC with LSCF to form the LSCF–GDC composite as the anode material has been applied for the direct oxidation

* Corresponding author. Tel.: +886 3 5716260; fax: +886 3 5715408.
E-mail address: tjhuang@che.nthu.edu.tw (T.-J. Huang).

0378-7753/$ – see front matter © 2010 Elsevier B.V. All rights reserved.
doi:10.1016/j.jpowsour.2010.11.012

of methane in intermediate-temperature SOFCs and shown to have no formation of carbon deposits [14]. Notably, the deposited carbon can form the coke, which causes a serious problem during direct oxidation of methane in the SOFCs [15]. Since CO can also form the deposited carbon via the disproportionation reaction of $2CO \rightarrow CO_2 + C$ [16], the LSCF–GDC composite was used as the anode material in this work. Additionally, since Ag can be used as the metal component in the anode cermets for the SOFCs using CO as the anode fuel for a better SOFC performance without carbon deposition [17,18], it is added to LSCF in this work to study the syngas reactivity.

On the other hand, doping Ag onto the A site of $La(CoFe)O_3$ to form $(LaAg)(CoFe)O_3$ (LACF) perovskite has shown to result in better CH_4 oxidation activity and much better CO oxidation activity than doping Sr [19]. Thus, it is interesting to compare the reactivity of LACF and Ag-added LSCF for electrochemical oxidation of syngas.

In this work, the syngas (H_2 + CO gas mixture with various H_2/CO ratios) was used as the anode fuel over LACF–GDC and Ag-added LSCF–GDC anodes, respectively. Both the current–voltage and the fixed-voltage measurements were performed and the results were in agreement with each other. The reactivity with H_2 as the fuel is larger than that with CO. The syngas reactivity increases with increasing H_2 content and that of Ag-added LSCF–GDC is better than that of LACF–GDC.

2. Experimental

2.1. Preparation of LACF–GDC and Ag-added LSCF–GDC powders

LACF was prepared by the glycine-nitrate process. Appropriate amounts of reagent-grade metal nitrates (Showa, Japan) $La(NO_3)_3{\cdot}6H_2O$, $Co(NO_3)_2{\cdot}6H_2O$, $Fe(NO_3)_3{\cdot}9H_2O$ and silver nitrate (Hwang Long, Taiwan) $AgNO_3$ were dissolved in de-ionized water. Glycine (Sigma, USA) was also dissolved in de-ionized water. Then, these two solutions were mixed with glycine to NO_3 ratio of 1:0.81. The mixture was heated under stirring to 120 °C and held until combustion occurred. The product was ground to powders and then calcined by heating at 5 °C min^{-1} to 500 °C and held for 2 h, then at 5 °C min^{-1} to 850 °C and held for 4 h. After cooling, the powders were screened and those with size smaller than 325 mesh were collected and then dried in an oven before usage. LACF of this work is $La_{0.7}Ag_{0.3}Co_{0.2}Fe_{0.8}O_{3-\delta}$.

LSCF was prepared also by the glycine-nitrate process as described in the above, except that $Sr(NO_3)_2$ (Showa, Japan) instead of $AgNO_3$ was used in preparation of the nitrate solution and the calcination temperature was 900 °C instead of 850 °C. LSCF of this work is $La_{0.58}Sr_{0.4}Co_{0.2}Fe_{0.8}O_{3-\delta}$.

Gadolinia-doped ceria (GDC) was prepared by co-precipitation. The details of the method have been presented elsewhere [20]. The GDC powders were calcined by heating at 10 °C min^{-1} to 400 °C and held for 2 h, and then at 10 °C min^{-1} to 800 °C and held for 4 h. After cooling, the powders were screened and those with size smaller than 325 mesh were collected. GDC of this work is $Ce_{0.9}Gd_{0.1}O_{1.95}$.

LACF–GDC composite powder was prepared by adding the above-prepared LACF and GDC powders in de-ionized water with stirring. The composition of LACF:GDC was 100:50 in weight. The mixture was ground for 24 h, then calcined by heating at 5 °C min^{-1} to 500 °C and held for 2 h, and then at 5 °C min^{-1} to 900 °C, held for 2 h. LSCF–GDC composite powder was prepared in the same way with LSCF:GDC being 100:50 in weight.

Ag-added LSCF–GDC powder was prepared by first dissolving $AgNO_3$ (Hwang Long, Taiwan) in de-ionized water and then adding the above-prepared LSCF and GDC powders with stirring. Then, the procedure was the same as described in the above. The loading of Ag was 2 wt% in terms of the weight of LSCF. Notably, Ag-added LSCF–GDC is also denoted as LSCF–GDC–Ag.

2.2. Construction of SOFC unit cell

A disk was cut from YSZ tape (156 μm thickness, Jiuhow, Taiwan) to make an electrolyte-supported cell. One side of the disk was spin-coated with the paste made of LSCF–GDC powders as the anode interlayer and then with LACF–GDC and LSCF–50GDC–Ag, respectively, to make the anode functional layer. The other side of the disk was spin-coated with LSCF–GDC as the cathode interlayer, then with 2 wt% Cu-added LSCF–GDC to make the cathode functional layer, and then with LSCF to make the current collecting layer. The details of the construction of the SOFC unit cell have been presented elsewhere [21].

2.3. Current–voltage measurement

The measurement of current–voltage curve was performed at 800 °C with pure hydrogen, pure CO or gas mixtures of H_2 and CO with various H_2/CO ratios flowing on the anode side and 20% O_2 in argon flowing on the cathode side. The gas flow rate was always 100 ml min^{-1}; the flow rates of anode and cathode gases were always the same. The flow rates of various components in the gas mixtures were measured by mass flow meters, respectively, before entering into a mixer. The overall flow rate was measured by a gas bubble meter at the outlet of the experimental setup. The voltage was varied by an adjustable resister, and both the voltage and the current were measured by a Multimeter (TES 2730).

2.4. Fixed-voltage measurement

The fixed-voltage measurements were performed at 0.6 V and 800 °C with 10% hydrogen, 10% CO or 10% (H_2 + CO) mixture with various H_2/CO ratios, all balanced by argon, flowing on the anode side and 20% O_2 in argon flowing on the cathode side. After the test, 10% O_2 in argon was passed over the anode side to detect any formation of CO_2 and/or CO due to carbon deposition during the syngas test. The flow rates were always 100 ml min^{-1}.

During the test, the electrical current, the voltage, and the outlet gas compositions were always measured. The compositions of CO and CO_2 were measured by CO-NDIR and CO_2-NDIR (non-dispersive infrared analyzer, Beckman 880), respectively. The composition of H_2 was measured by a gas chromatograph (China Chromatography 8900).

3. Results and discussion

3.1. Effect of the H_2/CO ratio on current–voltage performance

Fig. 1 shows that all values of the open circuit voltage are larger than 1.1 V; these values are close to the theoretical one and thus indicate that there should be no leakage in the setup of this work. When LACF–GDC is used as the anode material, the power density with pure H_2 as the anode fuel is larger or much larger than that with pure CO when the current density is close to or larger than that at the maximun power density. The maximum power density with the (H_2 + CO) syngas as the fuel is always larger than that with pure CO, as also shown in Table 1. The maximum power density increases upon increasing H_2 content in the syngas.

When LSCF–GDC–Ag, i.e. Ag-added LSCF–GDC, is used as the anode material, Fig. 2 shows that the power density with pure H_2 as the fuel is also larger than that with pure CO and this difference is larger than that with LACF–GDC anode. Table 2 shows that the maximum power density with pure H_2 is much larger than that with pure CO but smaller than that with the syngas of

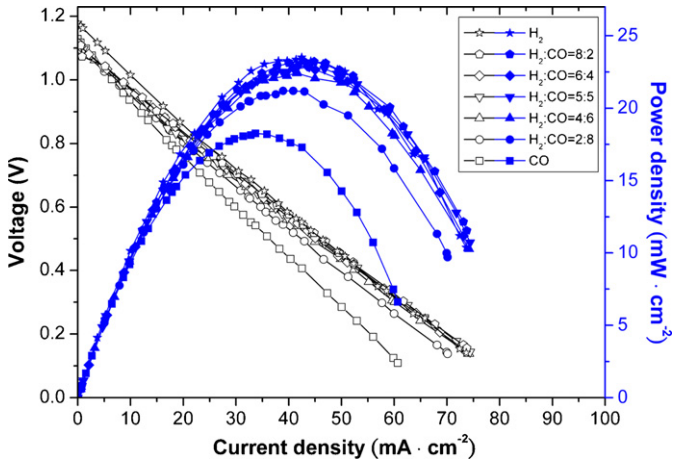

Fig. 1. Variation of voltage–current and power–current profiles with various 100% (H_2 + CO) mixture over LACF–GDC anode. Open symbol: voltage; filled symbol: power density.

Table 1
A comparison of open circuit voltage and maximum power density with various 100% (H_2 + CO) mixture over LACF–GDC anode.

Anode fuel	Open circuit voltage (V)	Maximum power density (mW cm^{-2})
100% H_2	1.179	23.50
H_2:CO = 8:2	1.117	23.25
H_2:CO = 6:4	1.114	22.90
H_2:CO = 5:5	1.114	22.87
H_2:CO = 4:6	1.113	22.47
H_2:CO = 2:8	1.105	21.20
100% CO	1.129	18.25

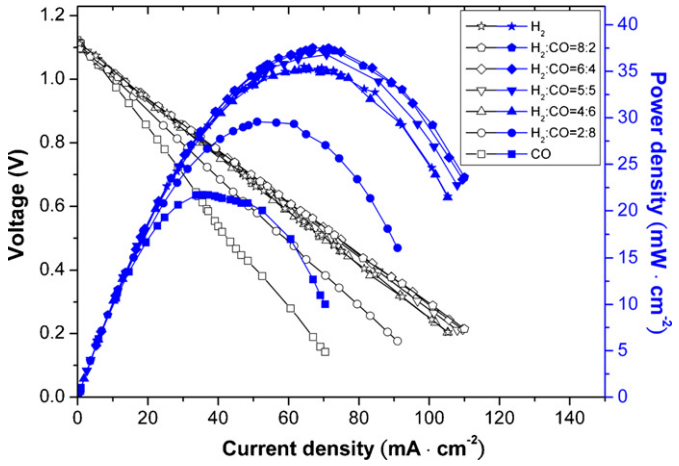

Fig. 2. Variation of voltage–current and power–current profiles with various 100% (H_2 + CO) mixture over LSCF–GDC–Ag anode. Open symbol: voltage; filled symbol: power density.

Table 2
A comparison of open circuit voltage and maximum power density with various 100% (H_2 + CO) mixture over LSCF–GDC–Ag anode.

Anode fuel	Open circuit voltage (V)	Maximum power density (mW cm^{-2})
100% H_2	1.121	35.50
H_2:CO = 8:2	1.102	37.53
H_2:CO = 6:4	1.109	37.31
H_2:CO = 5:5	1.109	36.78
H_2:CO = 4:6	1.107	35.29
H_2:CO = 2:8	1.110	29.48
100% CO	1.122	21.73

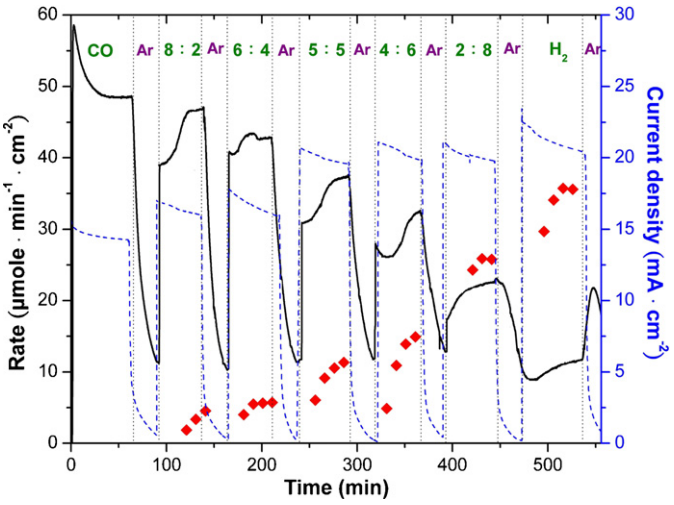

Fig. 3. Variation of CO_2 formation rate (—), H_2 consumption rate (♦) and measured current density (– – –) during fixed-voltage measurement with 10% (CO + H_2) mixture in argon over LACF–GDC anode upon decreasing CO content.

H_2:CO = 5:5–8:2. The maximum power density with the (H_2 + CO) syngas is also always larger than that with pure CO and increases when the H_2 content in the syngas increases.

The above-observed trend of the increase of the maximum power density upon increasing the H_2 content in the (H_2 + CO) syngas is a reverse of that as reported by Huang et al. [9], where the maximum power density decreases upon increasing the H_2 content. This is attributed to the fact that the LSCF/GDC ratio in this work is much larger than that in the work of Huang et al. [9]—that is, the LSCF/GDC ratio of the LSCF–GDC composite is 100:50 in this work, while it is 60:100 in the work of Huang et al. [9]. Notably, Huang et al. [9] have pointed out that, as the LSCF content in the LSCF–GDC composite increases, the H_2 reactivity increases but the CO reactivity decreases; restated, in the LSCF–GDC composite, LSCF favors the H_2 reactivity and GDC favors the CO reactivity. Therefore, when the H_2 content in the (H_2 + CO) syngas increases, the H_2 reactivity can become larger than the CO reactivity and the SOFC performance can become better, as observed for LSCF–GDC–Ag in this work. Since this behavior is also observed for LACF–GDC, the effect of GDC in the LACF–GDC composite on the reactivity can be the same as that in the LSCF–GDC composite.

3.2. *Effect of the H_2/CO ratio on the steady-state performance*

The steady-state performance was obtained by the fixed-voltage measurements. Notably, the steady-state performance can better represent the syngas reactivity during SOFC operation, which is usually at steady state with a fixed voltage or a fixed current, than the results obtained from the current–voltage measurement, which results in only initial-rate data.

Fig. 3 shows that, with the LACF–GDC anode during the fixed-voltage measurement, the current density with 10% CO as the fuel is much smaller than that with 10% H_2, as also shown by the averaged values of the measured current densities presented in Table 3. The current density with the syngas as the fuel is always larger than that with CO and increases upon increasing the H_2 content in the syngas. This trend of the SOFC performance in terms of the current density from the fixed-voltage measurement is the same as those in terms of the maximum power density from the current–voltage measurement. This indicates that the initial-rate data from the current–voltage measurement can represent the steady-state SOFC performance, at least for a comparison of the reactivity. Notably, the fixed-voltage measurement in this work

Table 3
Averaged values of measured current density at a fixed voltage of 0.6 V with various 10% (CO + H_2) mixture in argon over LACF–GDC and LSCF–GDC–Ag anodes.

Anode fuel	Measured current density (mA cm^{-2})	
	LACF–GDC	LSCF–GDC–Ag
10% H_2	20.80	31.30
H_2:CO = 8:2	20.45	34.37
H_2:CO = 6:4	20.16	34.13
H_2:CO = 5:5	20.06	33.25
H_2:CO = 4:6	17.09	31.13
H_2:CO = 2:8	16.64	27.64
10% CO	14.56	19.51

results in only quasi-steady state behavior due to possible occurrence of carbon deposition and anode reduction, as will be clarified latter.

Fig. 3 also shows that the rate of CO_2 formation decreases and that of H_2 consumption increases upon increasing the H_2 content in the syngas. The increase of the current density is in accordance with increasing H_2 consumption rate but with decreasing CO_2 formation rate, the latter being in accordance with decreasing CO content. Notably, CO_2 is also formed during argon (Ar) and H_2 flow; this indicates the presence of deposited carbon and thus the following reaction can occur:

$$C + 2O \rightarrow CO_2 \quad (6)$$

where the C species denotes deposited carbon and the O species denotes the surface lattice oxygen. The measured current density during Ar flow occurs due to the oxidation of the deposited carbon via reaction (6) with the lattice oxygen being formed via the reverse charge transfer reaction:

$$O^{2-} \rightarrow O + 2e^- \quad (7)$$

from the oxygen ion transported from the cathode. It is noted that the lattice oxygen may be formed over the surface to become the surface lattice oxygen, which can be directly utilized by reaction (6), or in the bulk to become the bulk lattice oxygen; in addition, the lattice oxygen in the bulk can be transported to the surface due to the oxygen mobility; thus, the bulk lattice oxygen can be indirectly utilized by reaction (6) via lattice oxygen extraction [22–25]. On the other hand, carbon deposition should have occurred via CO disproportionation:

$$2CO \rightarrow CO_2 + C \quad (8)$$

This may explain why the rate of CO_2 formation is not in accordance with the generation of the current density. This may also explain why the rate of CO_2 formation decreases with decreasing CO content.

Fig. 4 shows that, with LSCF–GDC–Ag anode during the fixed-voltage measurement and when the CO:H_2 ratio varies from 8:2 to 2:8, the behaviors of the current density, the CO_2 formation rate and the H_2 consumption rate are similar to those with LACF–GDC anode, respectively. Additionally, a comparison of Tables 2 and 3 for the LSCF–GDC–Ag anode shows that the trend of the measured current density is the same as that of the maximum power density—that is, the current density with 10% H_2 is much larger than that with 10% CO but smaller than that with the syngas of H_2:CO = 5:5–8:2. This again indicates that the initial-rate results obtained from the current–voltage measurement can represent, at least in some aspects, the steady-state SOFC performance.

3.3. Comparison of stability from anode reduction

The cyclic operation of 10% H_2 and pure Ar flow was carried out to compare the stability of LACF–GDC and LSCF–GDC–Ag as the anode materials in the H_2 atmosphere and with the occurrence

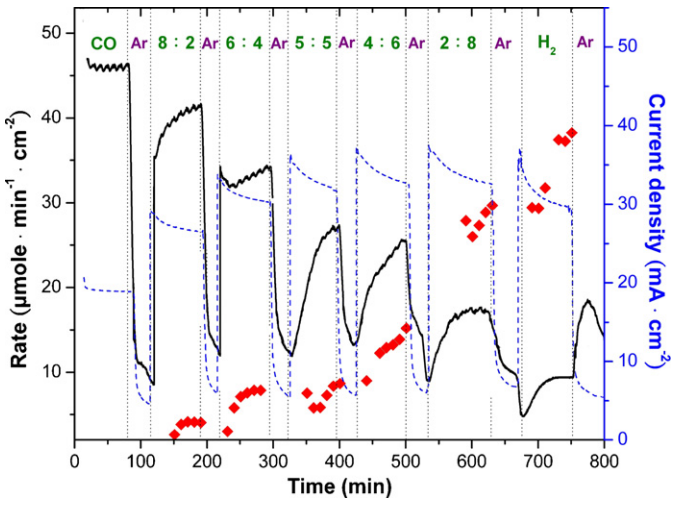

Fig. 4. Variation of CO_2 formation rate (—), H_2 consumption rate (♦) and measured current density (– – –) during fixed-voltage measurement with 10% (CO + H_2) mixture in argon over LSCF–GDC–Ag anode upon decreasing CO content.

of carbon deposition, both being able to cause anode reduction. Notably, the cyclic operations of Figs. 5 and 6 were carried out after the tests shown in Figs. 3 and 4, respectively; thus, some amount of deposited carbon may remain from previous carbon deposition via CO disproportionation. Fig. 5 shows that, over the LACF–GDC anode, the measured current density during the H_2 flow decreases dramatically after a cycle of H_2 and Ar flow. This is due to the deactivation of the SOFC performance by the anode deterioration from the reduction of its bulk lattice, whose occurrence is shown in the following. It is noted that CO_2 forms during Ar flow; this indicates the presence of deposited carbon and the occurrence of reaction (6), which removes the deposited carbon. In this work, the deposited carbon can be completely removed and thus does not cause permanent deactivation. Note also that reaction (6) consumes the O species, i.e. the lattice oxygen. The consumption of the lattice oxygen may result in the reduction of the anode bulk lattice if the current density is too small to supplement the bulk lattice oxygen via the oxygen ion transported from the cathode; this is the case for LACF–GDC during the Ar flow, as shown in Fig. 5.

The removal of deposited carbon frees the active sites and thus the H_2 consumption rate can increase after the Ar flow, as indeed

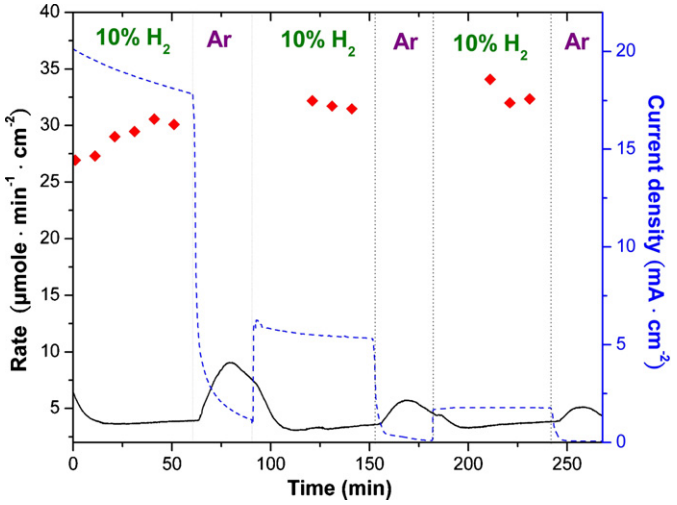

Fig. 5. Variation of CO_2 formation rate (—), H_2 consumption rate (♦) and measured current density (– – –) during fixed-voltage measurement with cyclic operation of 10% H_2 in argon and pure argon (Ar) over LACF–GDC anode.

Table 4
Averaged values of CO and CO_2 formation rates, and measured current density with cyclic operation of 10% H_2 in argon and pure argon (Ar) over LACF–GDC anode at a fixed voltage of 0.6 V.

		CO formation rate (μmole min^{-1} cm^{-2})	CO_2 formation rate (μmole min^{-1} cm^{-2})	Measured current density (mA cm^{-2})
Cycle 1	10% H_2	18.83	3.93	18.84
	Ar	5.54	7.19	1.76[a]
Cycle 2	10% H_2	3.69	3.77	5.52
	Ar	0.79	4.83	0.23[a]
Cycle 3	10% H_2	1.29	3.68	1.77
	Ar	0.47	4.49	0.13[a]

[a] Averaged values of current densities on stream 10–30 min after Ar flow.

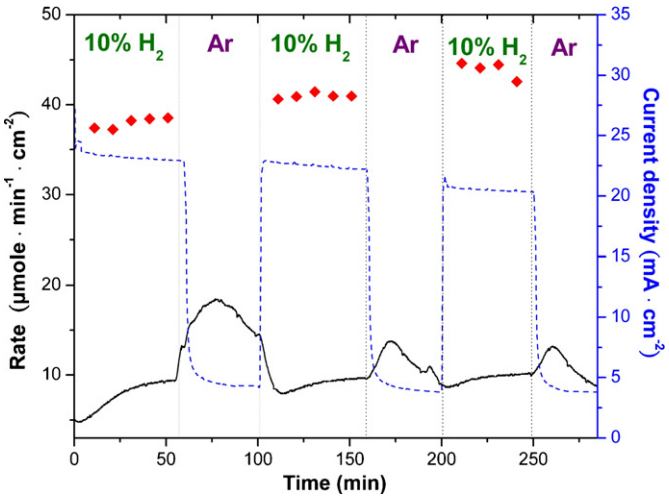

Fig. 6. Variation of CO_2 formation rate (—), H_2 consumption rate (♦) and measured current density (– – –) during fixed-voltage measurement with cyclic operation of 10% H_2 in argon and pure argon (Ar) over LSCF–GDC–Ag anode.

observed in Fig. 5. However, the decrease of the current density indicates that some O species for H_2 oxidation are not the surface lattice oxygen directly formed from the oxygen ion from the cathode, which should generate an electrical current according to reaction (7); instead, these O species should have been extracted from the anode bulk lattice [22–25]. Restated, the flowing of 10% H_2 results in the reduction of the anode bulk lattice; this may result in the deterioration of the anode material and thus the decrease of the SOFC performance. In fact, both CO and CO_2 activities as well as the measured current density during 10% H_2 flow decrease, as shown in Table 4. However, the reduction of the anode bulk lattice may also be a result of the removal of deposited carbon which consumes the O species; if some of these O species had been extracted from the anode bulk lattice, possible deterioration of the anode material may occur.

The formation of CO during either H_2 or Ar flow is attributed to oxidation of deposited carbon:

$$C + O \rightarrow CO \quad (9)$$

Table 4 also shows that the rate of CO foramtion decreases from cycle to cycle either during 10% H_2 flow or during Ar flow. This variation of the rate of CO formation is the same as that of CO_2 formation, indicating a decrease of the amount of deposited carbon. However, the rate of CO formation decreases dramatically from cycle to cycle while that of CO_2 formation does only moderately. The measured current density also decreases dramatically from cycle to cycle, indicating some relation between CO formation and generated current density—that is, the O species for CO formation via reaction (9) is the surface lattice oxygen directly formed from the oxygen ion from the cathode. Additionally, during the Ar flow, the rate of CO formation becomes much smaller than that of CO_2. However, the very small rate of CO formation is in accordance with the very small current density. This indicates again a relation between CO formation and generated current density. Note also that the rate of CO_2 formation is relatively constant but the measured current density decreases dramatically; this indicates that the formation of CO_2 via reaction (6) should have extracted the lattice oxygen from the anode bulk. Therefore, the formation of CO is associated with the current density while that of CO_2 is associated with the extraction of bulk lattice oxygen. The extraction of lattice oxygen from the anode bulk results in its reduction and possible deterioration of the LACF–GDC material and may explain the dramatic decrease of the measured current density after the Ar flow. Therefore, the deactivation of the SOFC performance may be explained by the anode deterioration due to the lattice oxygen extraction from the anode bulk by either H_2 or deposited carbon when the current density is too small to supplement the bulk lattice oxygen, being the case for LACF–GDC.

Fig. 6 shows that, over the LSCF–GDC–Ag anode, the measured current density with 10% H_2 flow decreases quite slightly from cycle to cycle, in comparison to the dramatic decrease over the LACF–GDC anode. This indicates that LSCF–GDC–Ag has better stability than LACF–GDC as the anode material in the H_2 atmosphere. It is noted that the CO_2 formation behavior during the Ar flow over the LSCF–GDC–Ag anode is similar to that over the LACF–GDC anode. However, Fig. 6 also shows that, when the flow shifts from H_2 to Ar during the first cycle, the drop of the current density is delayed after the onset of the Ar flow. This is attributed to a possible fact that some H species has been stored during the H_2 flow; thus, the current density is generated continuously after shifting to the Ar flow and drops only after the H species has been consumed. Notably, the

Table 5
Averaged values of CO and CO_2 formation rates, and measured current density with cyclic operation of 10% H_2 in argon and pure argon (Ar) over LSCF–GDC–Ag anode at a fixed voltage of 0.6 V.

		CO formation rate (μmole min^{-1} cm^{-2})	CO_2 formation rate (μmole min^{-1} cm^{-2})	Measured current density (mA cm^{-2})
Cycle 1	10% H_2	8.82	9.44	23.30
	Ar	0.16	11.93	4.50[a]
Cycle 2	10% H_2	7.22	9.66	22.47
	Ar	0.15	10.68	4.17[a]
Cycle 3	10% H_2	6.34	9.84	20.53
	Ar	0.05	10.67	4.18[a]

[a] Averaged values of current densities on stream 10–30 min after Ar flow.

phenomenon of the storage of the H species has been observed previously with the H species being the interstitial hydrogen species [26]. Additionally, Table 5 shows that the rate of CO_2 formation are rather constant during either the flow of 10% H_2 or that of Ar.

A comparison of Figs. 5 and 6 shows that, during the Ar flow, the measured current density over the LSCF–GDC–Ag anode is much larger than that over the LACF–GDC anode. Therefore, the supplementation of the lattice oxygen via reaction (7) can be faster over LSCF–GDC–Ag than that over LACF–GDC. Notably, some lattice oxygen formed via reaction (7) can be stored in the anode bulk lattice [22–25]. Thus, the extent of reduction of the anode bulk lattice of LSCF–GDC–Ag should be smaller than that of LACF–GDC; this may improve the stability of anode material, which may be confirmed by the very slight decrease of the measured current density for LSCF–GDC–Ag from cycle to cycle. This stabilizing effect may be attributed to the added Ag species. Figs. 5 and 6 also show that the CO_2 formation rate during the Ar flow is larger than that during the H_2 flow; however, the current density during the Ar flow is much smaller than that during the H_2 flow. This indicates that CO_2 formation via reaction (6) is favored by a smaller current density; restated, the formation of CO_2 should have extracted the lattice oxygen from the anode bulk. This again confirms the above explanation that the formation of CO_2 is associated with the extraction of bulk lattice oxygen while that of CO is associated with the current density. This can also explain the variation of the CO_2 formation rate versus the current density as shown in Figs. 5 and 6—that is, the rate of CO_2 formation is relatively small during the H_2 flow, when a relatively large current density is generated and thus the formation of CO is favored during the oxidation of deposited carbon, but relatively large during the Ar flow, when the generated current density is relatively small and thus the bulk latice oygen should be extracted for CO_2 formation.

4. Conclusions

The syngas has been tested as the anode fuel over LACF–GDC and Ag-added LSCF–GDC anodes, respectively. Both the current–voltage and the fixed-voltage measurements have been performed and the results are in agreement with each other. The reactivity with H_2 as the anode fuel is larger than that with CO. The reactivity increases with increasing H_2 content in the (H_2 + CO) syngas. Ag-added LSCF–GDC has better reactivity with H_2, CO and syngas as the anode fuel than LACF–GDC. Ag-added LSCF–GDC has better stability in H_2 atmosphere than LACF–GDC as the anode material. The deactivation of the LACF–GDC anode may be explained by the deterioration of the anode oxide structure due to the reduction of the anode bulk lattice, which is caused by the lattice oxygen extraction from the anode bulk by either H_2 or deposited carbon when the current density is too small to supplement the bulk lattice oxygen. Nevertheless, the deposited carbon can be completely removed and thus the anode may not be deactivated if the current density is high enough to supplement the bulk lattice oxygen so to keep the anode oxide structure.

References

[1] A. Weber, B. Sauer, A.C. Muller, D. Herbstritt, E. Ivers-Tiffee, Solid State Ionics 152–153 (2002) 543–550.
[2] T. Kivisaari, P. Bjornbom, C. Sylwan, B. Jacquinot, D. Jansen, A. de Groot, Chem. Eng. J. 100 (2004) 167–180.
[3] Y. Yi, A.D. Rao, J. Brouwer, G.S. Samuelsen, J. Power Sources 144 (2005) 67–76.
[4] J.P. Trembly, A.I. Marquez, T.R. Ohrn, D.J. Bayless, J. Power Sources 158 (2006) 263–273.
[5] J.P. Trembly, R.S. Gemmen, D.J. Bayless, J. Power Sources 163 (2007) 986–996.
[6] A.I. Marquez, T.R. Ohrn, J.P. Trembly, D.C. Ingram, D.J. Bayless, J. Power Sources 164 (2007) 659–667.
[7] J.P. Trembly, R.S. Gemmen, D.J. Bayless, J. Power Sources 169 (2007) 347–354.
[8] J.P. Trembly, R.S. Gemmen, D.J. Bayless, J. Power Sources 171 (2007) 818–825.
[9] T.J. Huang, C.L. Chou, W.J. Chen, M.C. Huang, Electrochem. Commun. 11 (2009) 294–297.
[10] A. Hartley, M. Sahibzada, M. Weston, I.S. Metcalfe, D. Mantzavinos, Catal. Today 55 (2000) 197–204.
[11] Y.H. Huang, R.I. Dass, Z.L. Xing, J.B. Goodenough, Science 312 (2006) 254–257.
[12] X.J. Chen, Q.L. Liu, S.H. Chan, N.P. Brandon, K.A. Khor, Electrochem. Commun. 9 (2007) 767–772.
[13] W.Z. Zhu, S.C. Deevi, Mater. Sci. Eng. A 362 (2003) 228–239.
[14] A. Sin, E. Kopnin, Y. Dubitsky, A. Zaopo, A.S. Aricò, L.R. Gullo, D. La Rosa, V. Antonucci, J. Power Sources 145 (2005) 68–73.
[15] J.B. Wang, J.C. Jang, T.J. Huang, J. Power Sources 122 (2003) 122–131.
[16] H. Nakano, S. Kawakami, T. Fujitani, J. Nakamura, Surf. Sci. 454–456 (2000) 295–299.
[17] F.Y. Wang, S. Cheng, B.Z. Wan, Catal. Commun. 9 (2008) 1595–1599.
[18] F.Y. Wang, G.B. Jung, A. Su, S.H. Chan, X. Hao, Y.C. Chiang, J. Power Sources 185 (2008) 862–866.
[19] K.S. Song, H.X. Cui, S.D. Kim, S.K. Kang, Catal. Today 47 (1999) 155–160.
[20] T.J. Huang, T.C. Yu, Catal. Lett. 102 (2005) 175–181.
[21] T.J. Huang, C.L. Chou, J. Electrochem. Soc. 157 (2010) P28–P34.
[22] T.J. Huang, M.C. Huang, Chem. Eng. J. 135 (2008) 216–223.
[23] T.J. Huang, M.C. Huang, J. Power Sources 175 (2008) 473–481.
[24] T.J. Huang, M.C. Huang, Chem. Eng. J. 138 (2008) 538–547.
[25] T.J. Huang, M.C. Huang, Int. J. Hydrogen Energy 34 (2009) 2731–2738.
[26] T.J. Huang, M.C. Huang, Int. J. Hydrogen Energy 33 (2008) 5073–5082.